ACS APPLIED MATERIALS & INTERFACES

Research Article

www.acsami.org

How to Prepare the Brightest Luminescent Coatings?

Géraldine Dantelle,* Blaise Fleury, Jean-Pierre Boilot, and Thierry Gacoin

Laboratoire de Physique de la Matière Condensée, UMR CNRS 7643 − Ecole Polytechnique, 91128 Palaiseau Cedex, France

Supporting Information

ABSTRACT: We address here the question of studying the parameters affecting the brightness of luminescent nanoparticulate coatings, among which are the absorption rate, the internal quantum yield of the phosphor nanoparticles, and the extraction factor of the emitted light in a solid angle perpendicular to the substrate. Experimental investigations are achieved on spray-deposited YVO_4:Eu particles, a system whose synthesis and properties are well documented so that particles of different sizes and microstructure can be considered. This allows a quantitative evaluation of the factors affecting film brightness. Considering a film made from raw colloidal particles, this work shows that its brightness is limited by a factor of 5 due to altered quantum yield of nanoparticles, a factor of 1.75 by dielectric effects and a factor of 2.4 by light extraction issues. This investigation, through providing quantitative evaluations of these different parameters, opens the way toward a possible rational design of inorganic luminescent coatings, with a possible improvement of brightness that could reach a factor of 30 as compared to simple films made directly from colloidal suspensions.

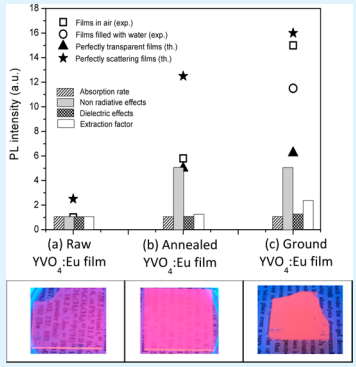

KEYWORDS: *luminescence efficiency, film, nanoparticle, scattering, extraction*

INTRODUCTION

Strongly luminescent films are required for numerous applications in the fields of lighting (organic light-emitting devices (OLEDs) and light-emitting diodes (LEDs)) or for the elaboration of display devices.[1−4] Film luminescence intensity is governed by three parameters: the film absorption rate, depending on the material absorption cross-section and the quantity of active material, the intrinsic luminescence quantum yield of the active material, and the extraction factor. The latter is specific to film structure and determines the quantity of emitted light which is effectively collected in the perpendicular direction of the film and can thus be used for applications. For example, in the transparent film presented in Figure 1a, a strong proportion of the luminescence is clearly guided into the film ($n_{film} \sim 1.65$) without being extracted from the top face of the film because of guiding effects. This is simply explained by dielectric effects and internal reflections at interfaces, as illustrated in Figure 1b which gives the relative proportions of directly emitted light I_{em} (I_{em} = 9% through each face, determined by the equation $(1 - \cos\theta_c)/2$ with the critical angle $\theta_c = \arcsin(n_{air}/n_{film})$ defined by the Snell-Descartes law), of light trapped in the substrate I_{trap} (I_{trap} = 40%, evaluated by $((1 - \cos\theta'_c)/2 - I_{em})*2$ with $\theta'_c = \arcsin(n_{sub}/n_{film})$; note that the multiplication by a factor of 2 takes into account light which is reflected at the film−air interface and goes into the substrate after the first reflection), and of guided light I_{guid} ($I_{guid} = 100 - 2I_{em} - I_{trap}$ = 42%). These calculations are performed for a perfectly transparent film with a refractive index n_{film} = 1.65 deposited on a substrate with a refractive index of n_{sub} = 1.5.

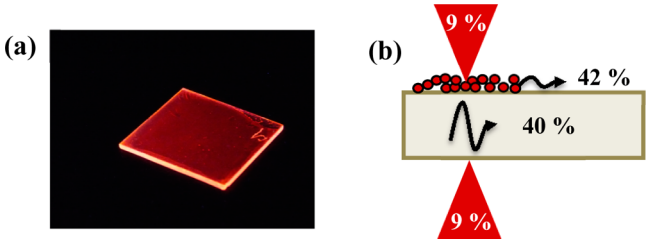

Figure 1. (a) Silica sol-gel film incorporating luminescent YVO_4 nanoparticles. (b) Illustration of a transparent film with a refractive index of 1.65 deposited onto a glass substrate with n = 1.5, with the fate of emitted light.

In order to optimize the different factors that govern film luminescence intensity, a great amount of work has been devoted to the search of efficient and photostable phosphors,[5,6] to the development of new film deposition methods enabling the deposition of a large quantity of matter,[7,8] and to the development of processes allowing light extraction, such as embedded scattering centers or surface patterning which modifies light propagation in transparent films.[9,10] In this context, we propose here to discuss the different contributions to film luminescence intensity and to quantify their impact on the collected intensity, with the aim of determining which parameter is the most important to elaborate the brightest luminescent films. The purpose is then to answer the question: how to get the strongest luminescence intensity from the top face of the films?

Received: August 22, 2013
Accepted: October 21, 2013
Published: October 21, 2013

   dx.doi.org/10.1021/am4035448 | ACS Appl. Mater. Interfaces 2013, 5, 11315−11320

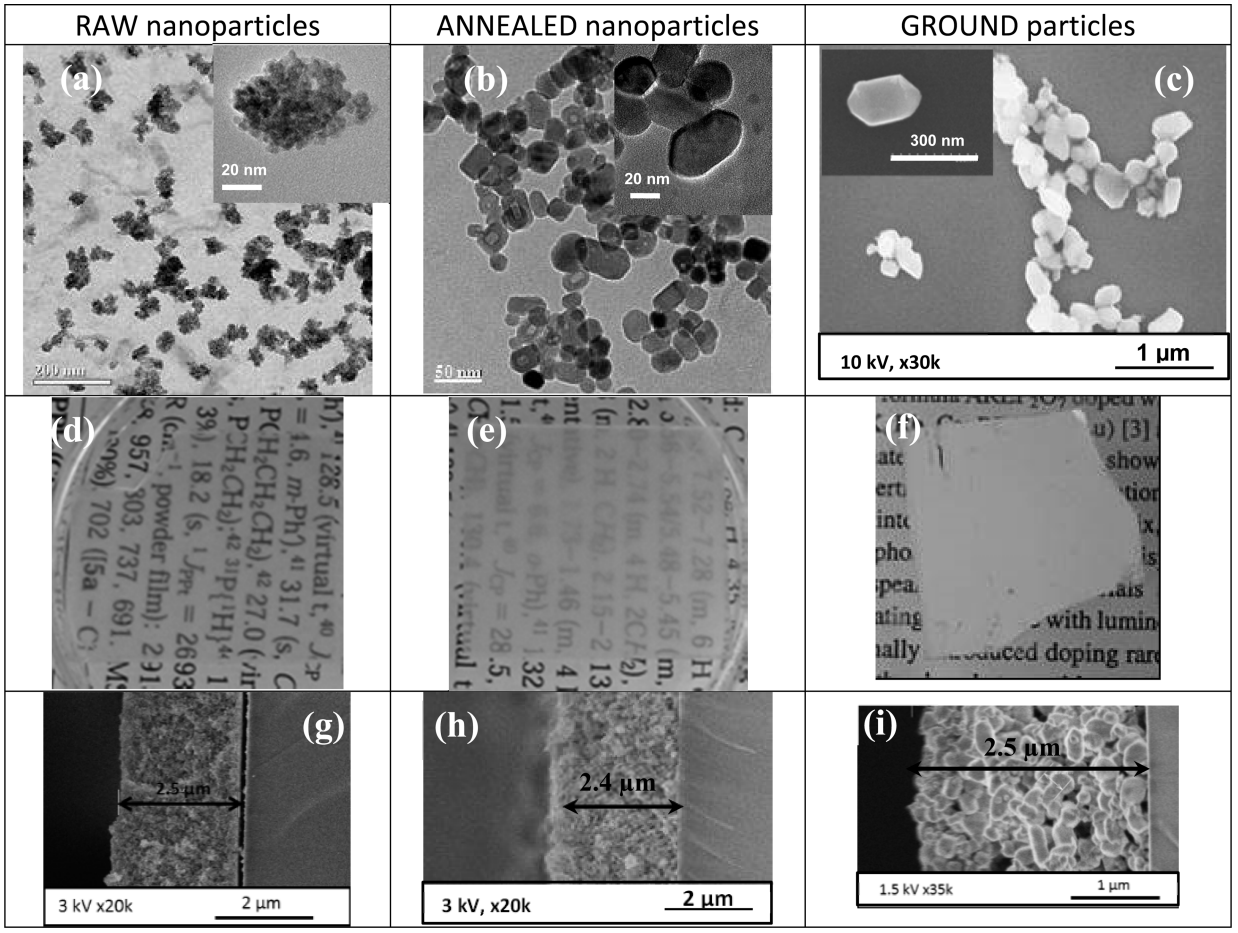

Figure 2. TEM (a, b) and SEM (c) images of the different YVO_4 particles. (d–f) Photographs of films made by spray-deposition of the different particles, under visible light. All films have been placed 2 cm above a text in order to visualize their scattering properties. Films have been cut to observe their cross sections (g–i) by SEM images and measure their thickness.

This study is based on films made of YVO_4 particles doped with 5 mol % trivalent europium ions. The choice for this compound is dictated by the fact that YVO_4 is a very well-known material, whose spectroscopic properties have been reported for many years and whose synthesis is well documented.[11−13] Bulk YVO_4:5%Eu can be synthesized by the solid state reaction of yttrium oxide and vanadium oxide above 1200°C and presents a luminescence quantum yield of 70 % for a 280 nm excitation.[14] Colloidal nanoparticles can be obtained by the coprecipitation of yttrium salt and orthovanadate in water at room temperature.[11] The morphology of the obtained particles consists in the aggregation of 7 nm sized primary grains, forming 40 nm nanoparticles, as observed in detailed microscopy studies (Figure 2a). The luminescence quantum yield of these particles is relatively low (8 % under a 280 nm excitation) due to the presence of structural defects and numerous −OH surface groups, both acting as traps for the luminescence and limiting the internal quantum yield of the nanoparticles. Thermal annealing allows one to increase the luminescence quantum yield but simultaneously induces particle growth. Thanks to a protected annealing process, the possibility to anneal the particles up to 1000°C without inducing the particle growth has been demonstrated.[15] The obtained particles, with an average size still centered at 40 nm, exhibit greatly improved optical properties, with a luminescence quantum yield of 40 %, as a result of their improved crystallinity (Figure 2b).[16] By considering the different relaxation pathways in the material, it has been shown that the discrepancy between the quantum yield of these annealed nanoparticles and the one of bulk material only comes from the difference of average refractive index of the dielectric media.[17]

As the purpose of this work is to prepare the brightest possible coatings, films were elaborated by spray-deposition of YVO_4:Eu colloidal solutions. The choice of this deposition technique lies in the fact that first it allows one to elaborate homogeneous films with a relatively high thickness (above 1 micrometer); second, it is very versatile, enabling the deposition of particles with different morphologies and size, as long as these particles can stay in suspension during the duration of the deposition technique. Finally, it avoids diluting the particles in a matrix, which contributes to an increase in the film brightness by increasing the quantity of matter. It can be also noted that the matrix could absorb part of the incident light, reducing the sample brightness. In the following, YVO_4:Eu particles of different size and morphology have been examined to determine the best conditions for the elaboration of the brightest films and to conclude on the most important parameter to play with to increase the light emitting performances of such coatings.

EXPERIMENTAL SECTION

Raw YVO_4 nanoparticles doped with 5 mol % europium were synthesized following the procedure detailed elsewhere.[11] Briefly $Y(NO_3)_3$ and $Eu(NO_3)_3$ salts were mixed together and slowly added

to a Na_3VO_4 solution under stirring at room temperature. A white precipitate is formed instantly. After a 30 min stirring, the precipitate is dialyzed against distilled water until the water conductivity goes down to 100 μS/cm. The obtained colloidal solution has a zeta potential of +6 mV. YVO_4:Eu nanoparticles are monodispersed, with an average size of 20 × 40 nm^2. In order to improve the optical properties of the obtained YVO_4 particles, a protected annealing procedure has been previously developed,[15] consisting of dispersing the nanoparticles in an amorphous silica matrix, annealing the nanocomposite up to 1000 °C, and removing the silica matrix by HF treatment to retrieve YVO_4:Eu nanoparticles in water. These nanoparticles are called "annealed nanoparticles". The obtained aqueous colloidal solution presents a zeta potential of +20 mV. It can be destabilized by dialyzing the solution against distilled water for 48 h. The resulting solution has a zeta potential of −1 mV.

Bulk YVO_4:Eu material was also synthesized by solid state reaction, according to the following route: $Y(NO_3)_3$ and $Eu(NO_3)_3$ were mixed together and NH_4OH (5M) was added to the solution. The yttrium and europium hydroxide precipitate was formed instantly. After drying, it was annealed at 1050 °C for 15 h in order to obtain the mixed oxide. This oxide powder was ground in an agate mortar with V_2O_5 and annealed at 1250 °C for 10 h to obtain YVO_4:Eu powder. Due to high temperature steps in the synthesis process, the obtained YVO_4:Eu powder is micrometer-sized; 1 g of YVO_4:Eu powder was then ground in 30 mL of ethyleneglycol using a planetary micro mill (Pulverisette 6 *classic line*, Fritsch) during 7 cycles of a 10 min grinding and a 5 min break. After the grinding process, the powder was washed 3 times in ethanol by centrifugation (11 363*g* for 20 min) and redispersed in ethanol. The obtained particles are polydispersed, with an average size of ∼300 nm. They are referred to as "ground particles".

Particles were characterized in solution, in terms of size and zeta potential, by Dynamic Light Scattering, using a Malvern instrument. Scanning electron microscopy was carried out using a SEM-FEG Hitachi S4800 microscope, using between 1 and 3 kV voltage.

Films were obtained by spray deposition using a Paasche Talon airbrush. The glass substrates were previously cleaned by a UV−ozone treatment. Typical sprayed volume and solution concentration are, respectively, 0.5 mL and 10 g/L, leading to 2.5 μm thick films. Prior to spray-deposition and during the deposition process, the substrates are heated at a temperature close to the boiling point of the solvent: for aqueous colloidal solution, the chosen temperature is 90 °C; for solutions in ethanol, the temperature is 60 °C.

Optical spectroscopy was performed using a spectrofluorimeter. The emission spectra were recorded either under a 280 or a 466 nm excitation. The lifetime measurements were obtained under a 280 nm excitation.

RESULTS AND DISCUSSION

Films have been elaborated by spraying colloidal solutions made of the hereafter particles:

- Raw nanoparticles (40 nm in average diameter), directly obtained by coprecipitation of nitrate and orthovanadate salts in water at room temperature (detailed synthesis has been reported elsewhere[11]). The zeta potential of the solution, which characterizes the stability of the particles in solution, is +6 mV.
- Annealed nanoparticles (40 nm in average diameter), obtained by annealing the above particles at 1000 °C according to the protected annealing process previously described. The zeta potential of the solution was measured to be +20 mV, meaning that these particles are more stable in solution than the raw nanoparticles.
- Ground particles resulting from the mild mechanical grinding of bulk YVO4:Eu material in ethyleneglycol. These well-faceted particles can be stabilized in ethanol. The synthesis method induces relatively high particle size distribution, with an average size around 300 nm, as determined by the size histogram given on Figure S1, Supporting Information, and obtained by analyzing the particle size by SEM. A SEM image of these particles is presented in Figure 2c.

By adjusting the particle concentration and the sprayed volume, films with a typical thickness of 2.5 micrometers were prepared from the different colloidal solutions. Photographs of the films are presented on Figure 2, as well as SEM cross sections. Films appear homogeneous over the whole substrate but present different scattering rates according to the type of sprayed particles. Considering the films of raw nanoparticles, the same scattering rates are observed for films with different thicknesses, up to 5 micrometers (Figure S2, Supporting Information), indicating that scattering comes from the film surface. Films of annealed particles behave the same way. The difference in terms of scattering between the film made of raw nanoparticles (characterized by a direct transmission at 800 nm of 90%) and the film made of annealed nanoparticles (characterized by a direct transmission at 800 nm of 40%) can be understood by taking into account the colloidal stability of the solutions: compared to raw nanoparticles, annealed nanoparticles form a more stable colloidal solution (zeta potential = +6 mV for the raw nanoparticle solution and +20 mV for the annealed nanoparticle solution). As previously shown for TiO_2 nanoparticles,[18] surface roughness is decreased when the stability of a sprayed colloidal solution decreases, due to a reduction of the particle mobility by aggregation.[19,20] This phenomenon induces a dramatic change in the surface scattering properties, as observed on the photographs (Fig 2). Regarding the film made of ground particles, strong scattering clearly originates from the film volume as films with different thicknesses present different scattering rates (Figure S3, Supporting Information).

Luminescence properties of the different films can be seen through excitation with a commercial 312 nm UV lamp excitation (Figure 3a−c), but for quantitative measurements, samples were excited at 280 nm, which is the optimum excitation wavelength. The luminescence intensity of the different films is reported in black empty squares in Figure 3.

In order to compare the optical properties of the different films, four factors that influence the film luminescence intensity can be listed: absorption rate, nonradiative effects within the particles, dielectric effects, and extraction factor. Nonradiative effects are intrinsic properties of the particles. They are related to the particle crystalline quality and can be estimated via the measurement of the luminescence quantum yield (QY) of these particles. Dielectric effects correspond to modifications of the refractive index in the local environment of the emitters and can be evaluated by the measurement of excited state lifetimes. Moreover, it is worth noting that, for an excitation at 280 nm, the incident beam is completely absorbed by the films, allowing a direct comparison of the luminescence intensity without taking into account any effect of the excitation. Indeed, as the absorption cross-section of YVO_4 at this wavelength is $\sigma_{280} = 10^{-17}$ cm^2, the whole incident radiation is absorbed over 500 nm, which is much inferior to the film thickness (2.5 micrometers), even when taking into account the porosity. For this reason, the histogram bar characterizing the absorption rate (Figure 3, diagonal lines) remains similar for all the samples. Thanks to different spectroscopic techniques (QY and lifetime measurements), contributions related to nonradiative effects and dielectric effects on film luminescence can be

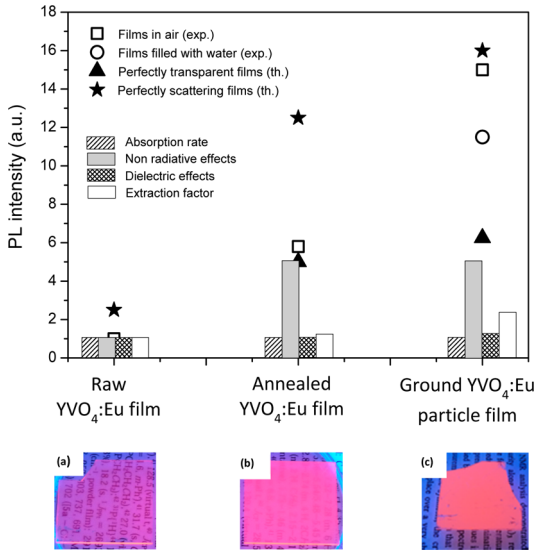

Figure 3. Black empty squares, film luminescence intensity at 618 nm, under a 280 nm excitation. It has been decomposed in four contributions represented by the histogram bars: absorption rate (diagonal lines), nonradiative effects on the intrinsic QY (grey), dielectric effects (crosshatched lines), and extraction factor (white). Triangles correspond to the expected luminescence intensity in the absence of scattering and stars to the expected luminescence intensity when considering a scattering that randomly redistribute lights in all the directions. The empty circle corresponds to the experimental luminescence intensity of the film made of ground particles filled with water. In addition, photographs under 312 nm of UV light of films made of raw nanoparticles (a), annealed nanoparticles (b) and ground particles (c), respectively, are inserted.

determined, allowing one to deduce the part that is attributed to the extraction via scattering.

Between a film of raw nanoparticles and a film of annealed nanoparticles, an increase of the luminescence intensity by a factor of 5.8 is measured, which can be partially explained by the difference of luminescence quantum yield between raw nanoparticles (Q.Y. = 8%) and annealed nanoparticles (Q.Y. = 40%), resulting from the removal of −OH surface traps and structural defects thanks to the thermal treatment.[17] Such effect of the thermal treatment can be also observed by measuring the $^5D_0$ excited state lifetime of Eu^{3+} in YVO_4 powder upon annealing temperature (Figure 4a). The annealed nanoparticles that have undergone a thermal treatment at 1000 °C present less surface traps and better crystallinity, enabling the lengthening of the $^5D_0$ lifetime and evidencing a reduction of the nonradiative de-excitation rate. In addition, to explain the difference of luminescence intensity between the film made of raw nanoparticles and the one made of annealed nanoparticles, one should take into account the extraction factor, governed here by the scattering. The difference of scattering rate between the two films (Figure 2d,e) can then be estimated to contribute to an increase in the luminescence intensity by an additional factor of 5.8 × 8/40 = 1.2 (corresponding to the ratio between the luminescence intensity increase of the films and the luminescence quantum yield increase of the nanoparticles).

An enhancement factor of 15 is observed between the film made of raw nanoparticles and the film made of ground particles. It can be decomposed as follows: a factor of 5 to take into account the reduction of the nonradiative effects due to the thermal annealing, a factor to consider the dielectric effects between nanoparticles and ground particles, and the rest, corresponding to the extraction factor, due to the increased scattering. The influence of the local refractive index was previously highlighted by G. Mialon et al.[17] showing that the luminescence quantum yield of bulk YVO_4 was 70% and that of annealed particles dispersed in water was only 40%, i.e., corresponding to a reduction of 1.75 due to dielectric effects.

As discussed in ref 21, the dielectric effects are directly related to the radiative lifetime as

$$\tau_{\mathrm{rad}}(n) = \left(\frac{1}{f(\mathrm{ED})}\right)\frac{{\lambda_0}^2}{\left(\frac{1}{3}(n^2+2)\right)^2 n} \quad (1)$$

with $f(\mathrm{ED})$ as the oscillator strength for the electric dipole transition, λ_0 as the wavelength in vacuum, and n as the refractive index of the dielectric medium. In agreement, we

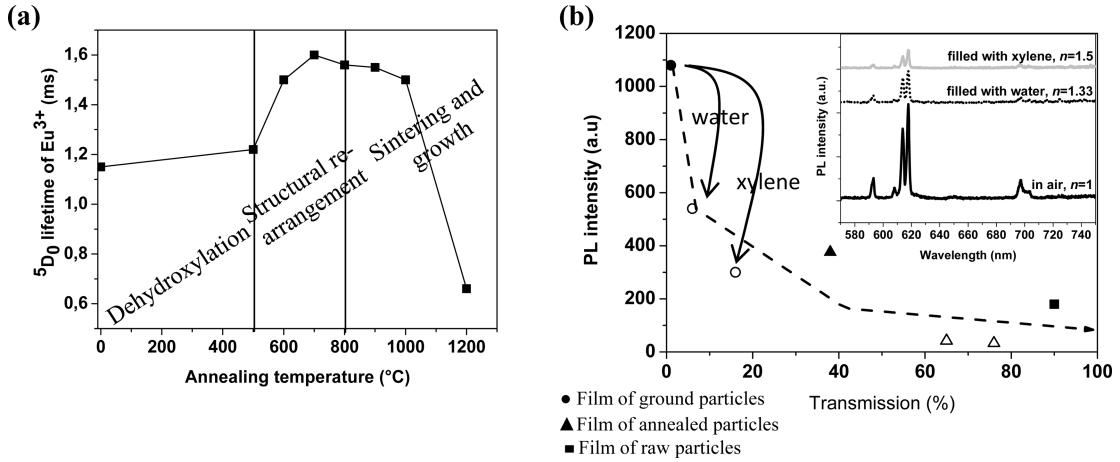

Figure 4. (a) Evolution of the $^5D_0$ lifetime of Eu^{3+} in the YVO_4 matrix with the annealing temperature. The lifetime has been measured at 618 nm for a 280 nm excitation. (b) Luminescence intensity at 618 nm versus film transmission at 800 nm. Data have been normalized by the quantum yield of the particles to highlight only the effect of film transmission. Data obtained directly with the films are represented with filled symbols; data obtained by filling the film pores to modify the film transparency are represented by empty symbols. The dashed line is a guide for the eyes. In the inset, the luminescence spectra of films made of ground particles and filled with air (solid line), with water, n = 1.33 (dashed line), and with xylene, n = 1.5 (grey line), under a 466 nm excitation are reported.

observe here a drastic decrease of the $^5D_0$ lifetime of Eu^{3+} in bulk YVO_4:Eu powder resulting from an annealing at 1200 °C, with τ_P = 0.63 ms (Figure 4a).

The lifetime of the film of ground particles (τ_{GP} = 0.89 ms) is higher than the one of the bulk YVO_4:Eu powder (τ_P = 0.63 ms). Considering all the other contributions to the lifetime (nonradiative effect, transfer between vanadate and Eu ions, etc.[17]) similar for these two materials, it indicates a smaller local refractive index in the film of ground particles than in the bulk, due to the reduced size of the particles. From those Eu^{3+} lifetime measurements, considering the ratio τ_{GP} over τ_P and the refractive index of bulk YVO_4 (n_{YVO4} = 2), the average refractive index of the film made of ground particles can be estimated to be 1.8.

Thus, the dielectric effects in the film of ground particles (n = 1.8) are not as important as in the bulk YVO_4:Eu powder (n = 2), for which an enhancement factor of 1.75 was demonstrated with respect to the nanoparticles.[17] Taking into account the ratio between τ_{GP} and τ_P, we thus estimate that the dielectric effects in the ground particle film are responsible for an increase of the luminescence intensity by a factor of $1.75 \times (\tau_P/\tau_{GP})$ = 1.25 with respect to the nanoparticles.

Accordingly, we deduce that the extraction factor leads to an increase of the film luminescence intensity by a factor of 2.4 (Figure 3). Taking into consideration the geometry and reflections at the interfaces of a film with a refractive index of 1.65 and considering that the scattering redistributes the light in all directions in an isotropic manner, a maximum extraction factor can be determined as follows: without scattering, only 9% of light is extracted from the top face of the film, and with scattering, half of the 42% of guided light is additionally extracted, leading to an extraction factor of $(42/2 + 9)/9 = 3.3$, with respect to a completely transparent film. When filling the film with water, this extraction factor is reduced, leading to a decrease of the film intensity from 15 to 11.5 (Figure 3, empty circle). Depending on the extraction factor, film intensity can vary between the extreme values indicated in Figure 3 by stars (for completely scattering films) and by triangles (for completely transparent films).

It is worth noting that the deposition of bigger particles would enable one to take advantage of stronger dielectric effects (up to 1.75), but another deposition technique should be envisaged as such particles would sediment rapidly due to their size, preventing their spray-deposition. Finally, we consider the case where only a small fraction of the excitation radiation is absorbed by the films. Film luminescence intensity has been thus investigated under an excitation at 466 nm, i.e., in a f−f intra-configurational transition of Eu^{3+} which presents an absorption cross-section of $\sigma_{466} = 1.4 \times 10^{-21}$ cm^2. In these conditions, only a few percent of the excitation radiation is absorbed over the film thickness (2.5 μm).

Luminescence of the different films is reported in Figure 4b (full circles) as a function of their direct transmission at 800 nm. It is worth noting that data have been normalized by the quantum yield of the particles and the film density in order to highlight only the effect of scattering. Films of ground particles and of annealed nanoparticles have also been filled with liquids of different refractive index, showing a different scattering rate. Their luminescence intensity is presented as empty circles in Figure 4b, and in the inset, the spectra corresponding to the film made of ground particles in different media are reported.

Strong variation of the luminescence intensity is observed with the scattering rate, with a difference of luminescence intensity up to a factor of 30. In the case of an excitation at 466 nm where not all incident radiation is absorbed within the film thickness, the increased scattering efficiency strongly modifies the light path. Hence, when strong scattering occurs, the excitation radiation remains longer in the film, allowing a better excitation and much stronger film emission intensity. To get very bright coatings, the scattering factor is all the more important given that the absorption rate is low.

CONCLUSION

Through this study, we show that, when considering films with a total absorption of the incident light, the intrinsic properties of the active materials play a key role in the optimization of the film luminescence intensity. Indeed, by improving the structural properties of raw YVO_4:Eu, we manage to improve the luminescence intensity of the films by a factor of 5. This enhancement factor can even reach 6 when taking into account dielectric effects and depositing 300 nm particles. However, in conditions for which the absorption rate is limited, the key parameter to optimize is the scattering rate, allowing one to enhance both the extraction factor and the optical path of the incident light. In those conditions, we show an enhancement factor up to 30 on the film luminescence intensity.

For some particular applications, transparency property can be additionally required. Transparent films can be obtained, in particular by reducing the particle size and decreasing their mobility,[18] but one should expect a decrease of the luminescence intensity by a factor of 3.3 (estimated by taking into account total reflections at the interfaces for films with n = 1.65) in the case when all incident light is absorbed and an even stronger decrease if the excitation is only partially absorbed. In such cases, it can be very useful to add a surface patterning to efficiently couple light to the film.[10,22,23]

ASSOCIATED CONTENT

Supporting Information

Details on size distribution of ground particles and on film transmission spectra. This information is available free of charge via the Internet at http://pubs.acs.org.

AUTHOR INFORMATION

Corresponding Author

*E-mail: geraldine.dantelle@polytechnique.edu.

Notes

The authors declare no competing financial interest.

REFERENCES

(1) Yum, J. H.; Seo, S. Y.; Lee, S.; Sung, Y. E. *J. Electrochem. Soc.* **2003**, *150*, H47−H52.

(2) Wu, H.; Zhou, G.; Zou, J.; Ho, C. L.; Wong, W. Y.; Yang, W.; Peng, J.; Cao, Y. *Adv. Mater.* **2009**, *21*, 4181−4184.

(3) Krummacher, B. C.; Choong, V. E.; Mathai, M. K.; Choulis, S. A.; So, F.; Jermann, F.; Fiedler, T.; Zachau, M. *Appl. Phys. Lett.* **2006**, *88*, 113506.

(4) Luo, H.; Kim, J. K.; Schubert, E. F.; Cho, J.; Sone, C.; Park, Y. *Appl. Phys. Lett.* **2008**, *86*, 243505.

(5) Im, W.B.; Brinkley, S.; Hu, J.; Mikhailovsky, A.; DenBaars, S. P.; Seshadri, R. *Chem. Mater.* **2010**, *22*, 2842−2849.

(6) Yan, B.; Xu, S.Q. *Opt. Mater.* **2007**, *29*, 547−551.

(7) Burgin, J.; Jubera, V.; Debeda, H.; Glorieux, B.; Garcia, A.; Lucat, C. *J. Mater. Sci.* **2011**, *46*, 2235−2241.

(8) Bauer, E.; Mueller, A. H.; Usov, I.; Suvorova, N.; Janicke, M. T.; Waterhouse, G. I. N.; Waterland, M. R.; Jia, Q. X.; Burrell, A. K.; McCleskey, T. M. *Adv. Mater.* **2008**, *20*, 4704−4707.

(9) Ko, K. Y.; Lee, Y.; Do, Y. R.; Huk, Y. D. *J. Appl. Phys.* **2007**, *102*, 013509.
(10) Revaux, A.; Dantelle, G.; Decanini, D.; Haghiri-Gosnet, A. M.; Weisbuch, C.; Gacoin, T.; Boilot, J. P.; Benisty, H. *Nanotechnology* **2011**, *22*, 365701.
(11) Huignard, A.; Gacoin, T.; Boilot, J. P. *Chem Mater.* **2000**, *12*, 1090−1094.
(12) Huignard, A.; Buissette, V.; Franville, A. C.; Gacoin, T.; Boilot, J. P. *J. Phys. Chem B* **2003**, *107*, 6754−6759.
(13) Capobianco, J. A.; Kabro, P.; Ermeneux, F. S.; Moncorgé, R.; Bettinelli, M.; Cavalli, E. *Chem. Phys.* **1997**, *214*, 329−340.
(14) Riwotzki, K.; Haase, M. *J. Phys. Chem. B* **1998**, *102*, 10129−10135.
(15) Maurin, I.; Dantelle, G.; Boilot, J. P.; Gacoin, T. *J. Mater. Chem. C* **2013**, *1*, 13−22.
(16) Mialon, G.; Gohin, M.; Gacoin, T.; Boilot, J. P. *ACS Nano* **2008**, *2*, 2505−2512.
(17) Mialon, G.; Turckan, S.; Alexandrou, A.; Gacoin, T.; Boilot, J. P. *J. Phys. Chem. C* **2009**, *113*, 18669−18706.
(18) Fleury, B.; Dantelle, G.; Darbe, S.; Boilot, J. P.; Gacoin, T. *Langmuir* **2012**, *28*, 7639−7645.
(19) Deegan, R. D.; Bakajin, O.; Dupont, T. F.; Huber, G.; Nagel, S. R.; Witten, T. A. *Nature* **1997**, *389*, 827−829.
(20) Yunker, P. J.; Still, T.; Lohr, M. A.; Yodh, A. G. *Nature* **2011**, *476*, 308−311.
(21) Meltzer, R. S.; Feofilov, S. P.; Tissue, B.; Yuan, H. B. *Phys. Rev. B: Condens. Matter* **1999**, *60*, R14012.
(22) Bermel, P.; Luo, C.; Zeng, L.; Kimerling, L. C.; Joannopoulos, J. D. *Opt. Express* **2007**, *15*, 16986−17000.
(23) Lee, S.; Wrzesniewski, E.; Cao, W.; Xue, J.; Douglas, E. P. *J. Disp. Technol.* **2013**, *9*, 497−503.